

PDF hosted at the Radboud Repository of the Radboud University Nijmegen

The following full text is a publisher's version.

For additional information about this publication click this link.

<http://hdl.handle.net/2066/116997>

Please be advised that this information was generated on 2020-10-24 and may be subject to change.

Fine structure of the lowest Landau level in suspended trilayer graphene

H. J. van Elferen,¹ A. Veligura,² N. Tombros,² E. V. Kurganova,¹ B. J. van Wees,² J. C. Maan,¹ and U. Zeitler^{1,*}

¹*High Field Magnet Laboratory and Institute for Molecules and Materials, Radboud University Nijmegen, Toernooiveld 7, 6525 ED Nijmegen, The Netherlands*

²*Physics of Nanodevices, Zernike Institute for Advanced Materials, University of Groningen, Nijenborgh 4, 9747 AG Groningen, The Netherlands*

(Received 28 March 2013; published 9 September 2013)

Magnetotransport experiments on ABC-stacked suspended trilayer graphene reveal a complete splitting of the 12-fold degenerated lowest Landau level, and, in particular, the opening of an exchange-driven gap at the charge neutrality point. A quantitative analysis of distinctness of the quantum Hall plateaus as a function of field yields a hierarchy of the filling factors: $\nu = 6, 4$, and 0 are the most pronounced, followed by $\nu = 3$, and finally $\nu = 1, 2$, and 5 . Apart from the appearance of a $\nu = 4$ state, which is probably caused by a layer asymmetry, this sequence is in agreement with Hund's rules for ABC-stacked trilayer graphene.

DOI: [10.1103/PhysRevB.88.121302](https://doi.org/10.1103/PhysRevB.88.121302)

PACS number(s): 73.22.Pr, 71.70.Di, 73.43.-f

The unconventional quantum Hall effects observed in single-layer graphene (SLG),^{1,2} bilayer graphene (BLG),³ and trilayer graphene (TLG)⁴⁻⁸ are a hallmark for the relativistic band structure in this intriguing material. Considering only nearest-neighbor interactions, the Landau-level spectrum of all these forms of N -layer graphene can be described by a $4N$ -fold degenerate zero-energy level, shared equally between electrons and holes, and fourfold degenerate higher Landau levels for electrons and holes separately.⁹⁻¹¹ When taking more than only interlayer coupling into account, the situation becomes more complicated. In particular, for trilayer graphene the two possible stacking sequences ABA and ABC lead to different band structures¹² and a distinctly different Landau-level spectrum.^{4,6-8,13}

In a magnetic field, exchange effects and the Zeeman splitting can lift this degeneracy.¹⁴ However, the mobility in standard samples deposited on a SiO₂ substrate is in general too low in order to resolve such effects. Only when replacing the SiO₂ substrate by, e.g., hexagonal boron nitride (hBN),^{15,16} or by fully suspending the device from the substrate,^{17,18} does the mobility become high enough to completely resolve the fine structure of the lowest Landau level.

In this Rapid Communication we present magnetotransport experiments on a suspended ABC-stacked TLG sample. This system is known to display an unconventional quantum Hall effect (QHE) with a 12-fold degenerate lowest Landau level and a Berry phase of 3π .⁵⁻⁸ We show that a quantizing magnetic field fully lifts this 12-fold degeneracy. Furthermore, we established a hierarchical order of the related filling factors: $\nu = 6, 4$, and 0 are the most pronounced, followed by $\nu = 3$, and finally $\nu = 1, 2$, and 5 .

We have prepared a suspended TLG sample using an acid free method.¹⁸ Following standard techniques,¹⁹ we first exfoliated flakes from highly oriented pyrolytic graphite and deposited them on a Si/SiO₂ substrate covered with a 1.15 μm thick LOR-A resist (MicroChem Corp.) layer. The TLG flake was then identified by its thickness measured through its optical contrast.²⁰ Subsequently, two electron beam lithography steps were performed in order to contact the flake with Ti-Au contacts and to remove part of the LOR-A below the graphene flake. The resulting device is a freely suspended bridge, 0.5 μm

wide and 1.3 μm long, across a trench formed in the LOR-A with two metallic contacts on each side. Carriers in the sample are induced by applying a back-gate voltage V_G on the highly n -doped Si wafer yielding a carrier concentration $n = \alpha V_G$. The lever factor $\alpha \approx 1 \times 10^{14} \text{ m}^{-2} \text{ V}^{-1}$ is determined experimentally from the positions of the filling factors in Fig. 1 and agrees within a factor of 2 with that deduced from the geometric gate capacitance of the device before annealing.

Measurements were performed at low temperatures and high magnetic fields up to 30 T using a low-frequency (1.87 Hz) lock-in technique with an excitation current $I \leq 1 \text{ nA}$. The sample was mounted on an *in situ* tilting stage where the angle ϕ between the total magnetic field B_{tot} and the perpendicular component $B_{\perp} = B \cos(\phi)$ can be controlled independently. ϕ was determined using the Hall resistance of a second sample on the same substrate. The device was slowly cooled down to 4.2 K and current annealed²¹ by applying a dc bias current up to 3 mA. The local annealing resulted in a high quality sample where the charge neutrality point (CNP) is centered around zero gate voltage.

In Fig. 1 we show the two-terminal conductance G of our sample as a function of V_G in a perpendicular magnetic field ($\phi = 0$). Before calculating the conductance, we have subtracted a constant background resistance of 550 Ω originating from the finite contact and lead resistance from the measured two-terminal resistance. Using the slope of the dashed line in the figure, $G = ne\mu w/l$, we estimate a zero-field mobility $\mu \approx 8 \text{ m}^2/\text{Vs}$ around the CNP. Here $l = 1.3 \mu\text{m}$ and $w = 0.5 \mu\text{m}$ are the length and the width of the sample and we assume that their ratio did not change significantly during annealing. A value of the order of a few m^2/Vs for the mobility is further confirmed by the fact that we start entering the quantum Hall regimes already around 1 T (see below).

At $B < 3 \text{ T}$, quantum Hall plateaus at filling factors $\nu = 4$ and $\nu = 6$ already start to develop. A further increase of the magnetic field up to 10 T results in the complete lifting of the lowest Landau level and the formation of quantized Hall plateaus at filling factors $\nu = 5, 3, 2$, and 1 .

The conductance G is the inverse of the resistance R , which is determined by a combination of the magnetoresistance

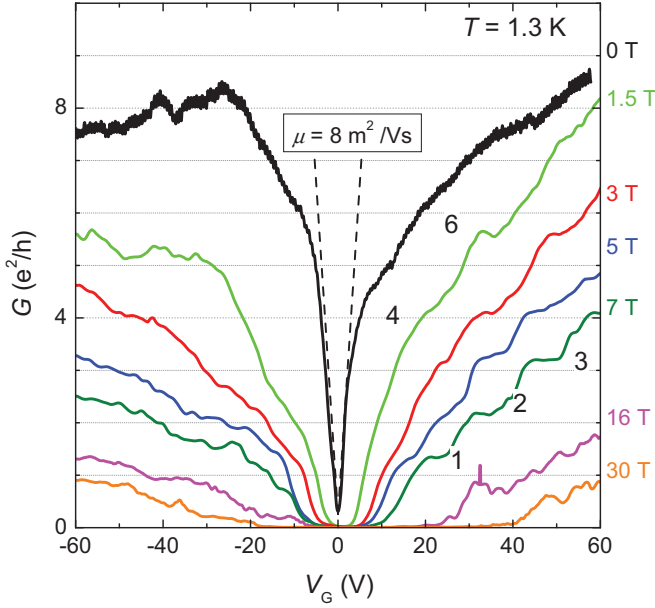


FIG. 1. (Color online) Conductance traces at $T = 1.3$ K for magnetic fields between 0 and 30 T. The dashed line through the 0 T data is used to estimate the device mobility. The numbers indicate the quantization of G in integer units of e^2/h .

R_{xx} and the Hall resistance R_{xy} (after subtraction of contact and lead resistances). Our data for high concentrations show that R is dominated by R_{xy} , indicated by the formation of plateaus in Fig. 1. Motivated by the empiric relation $R_{xy} \propto B \times dR_{xx}/dB$,^{22,23} and in order to accentuate the plateaus more clearly we define therefore a normalized derivative,

$$D = -V_G \frac{dR}{dV_G}, \quad (1)$$

which is plotted in Fig. 2(a) for the measured data in Fig. 1. In this way, plateaus in R , originating from R_{xy} , result in clear minima at integer filling factors $\nu = ne/hB$ that are related to Shubnikov–de Haas minima in R_{xx} . These minima are well pronounced on the electron side, $V_G > 0$ [see the dashed lines in Fig. 2(a)]. On the hole side, a changing background resistance, possibly originating from less well-annealed parts of the sample, makes it harder to distinguish the different plateaus and corresponding minima, though they still remain visible. Therefore, we will focus our analysis on the electron side only.

In Fig. 2(b) we plot the position of the minima in D as a function of gate voltage (proportional to n). As expected, they show a linear magnetic field dependence. The finite offset at zero field is probably caused by the persistence of the quantized states down to zero field.^{24,25}

We now focus on the quantitative development of filling factors $\nu = 6, 4, 3, 2$, and 1 by determining a typical magnetic field B_0 at which quantization appears. As can be seen in Fig. 2(a), the oscillation amplitude increases with increasing field until fully developed plateaus appear in G . We use a quantitative analysis of the amplitudes A_ν similar to the determination of the Dingle temperature T_D in Ref. 26. This model is based on the Lifshitz-Kosevich formula,²⁷ $\Delta R = A_\nu(B, T) \sin(P/B + \varphi)$, with an oscillation amplitude

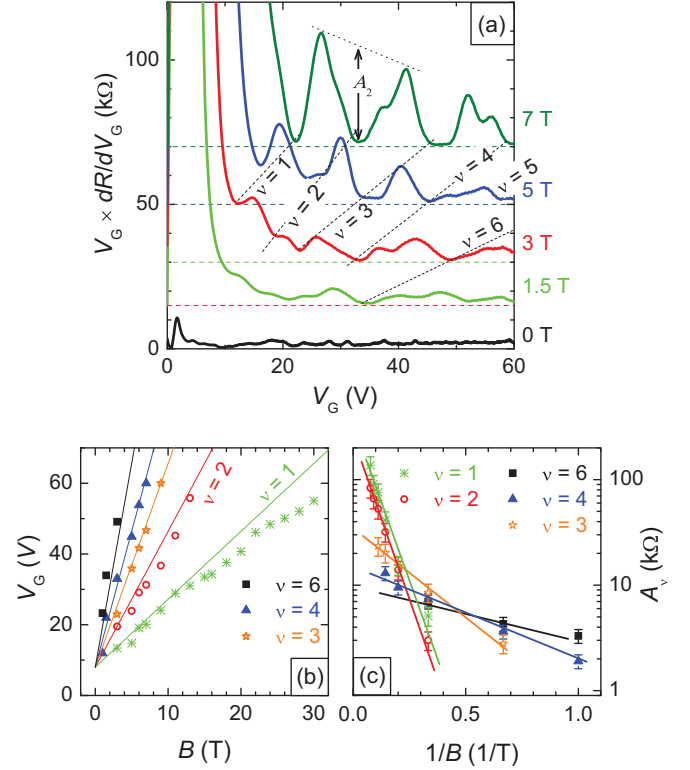


FIG. 2. (Color online) (a) Derivative $D = V_G \times dR/dV_G$ for magnetic fields between 0 and 7 T. Curves are shifted upwards proportional to the magnetic field value. The dashed lines mark the position of the minima in D with the corresponding filling factor. The arrow illustrates the definition of the oscillation amplitude A_ν at $\nu = 2$. (b) Gate-voltage positions of the minima in D as a function of field. The lines indicate the expected linear behavior for the given filling factors. (c) Oscillation amplitude A_ν as a function of $1/B$ for the different filling factors.

$A_\nu(B, T)$, a period P , and a phase φ . Depending on the corresponding gap at a given filling factor ν , the amplitude is different for different ν . $A_\nu(B, T)$ contains a temperature dependent term R_T and a field dependent Dingle term R_D . In order to concentrate on the field dependence alone, we have performed all measurements at a constant temperature $T = 1.3$ K, i.e., leaving R_T constant for all measurements.

In a regime where two neighboring Landau levels are still overlapping, the Dingle factor at the oscillation minima scales as $R_D \propto \exp(-B_0/B)$. For higher fields, where the levels are fully separated, R_D saturates and becomes field independent. Filling factors with the largest excitation gap appear first at the lowest B , while filling factors corresponding to smaller gaps appear at higher B . Quantitatively, using the above equation, we define an onset field B_0 where 37% ($1/e$) of the maximum oscillation amplitude is reached.

In Fig. 2(c) we plot the amplitude A_ν , [defined as the distance from the oscillation minimum to the average of the two neighboring maxima—see the arrow in Fig. 2(a)] as a function of $1/B$ for the different filling factors. The solid lines indicate the slope of the data points and determine the values of B_0 summarized in Table I. The $\nu = 5$ minimum just starts to appear in the 5 T trace in Fig. 2(a); due to the limited

TABLE I. Field values B_0 characterizing the strength of the plateaus at $\nu = 6, 4, 3, 2$, and 1 .

ν	6	4	3	2	1
B_0 (T)	1.4 ± 0.5	2.2 ± 0.5	4 ± 1	14 ± 2	14 ± 2

gate voltage range we were not able to perform a quantitative analysis of its amplitude $A_5(B)$.

As stated above, the values of B_0 in Table I describe a hierarchy of the filling factors. The most pronounced filling factor is found to be $\nu = 6$, separating the lowest 12-fold degenerate Landau level of ABC-stacked TLG from the first Landau level. It confirms that our sample is indeed TLG.⁵⁻⁸ The subsequent filling factors are related to the lifting of the degeneracy of the lowest Landau level: first $\nu = 3$ and at higher fields $\nu = 1, 2$, and 5 , a sequence which is in agreement with Hund's rules of ABC-TLG.^{28,29} However, filling factor $\nu = 4$ is also observed experimentally in this sequence whereas it is not predicted by Hund's rules for ABC-TLG. We attributed its appearance to a layer asymmetry caused by an external electric field of the back gate or local inhomogeneities.¹³

Additionally, a field-induced gap opens at the CNP, as theoretically expected for ABC-stacked TLG but not for ABA-stacked TLG.^{12,28,30} We analyze the nature of this gap in more detail by focusing on the diverging resistance at the CNP. Already at zero magnetic field a strong activated temperature dependence is observed [see Fig. 3(a)]. It can be described by $R_{\text{CNP}} \propto \exp(\Delta_0/k_B T)$, with a gap size $\Delta_0 \approx 0.38$ meV. In a magnetic field, R_{CNP} grows rapidly with increasing B/T , suggesting an increase of the relevant gap. For B/T up to 0.5 T/K the roughly exponential behavior of R_{CNP} suggests an Arrhenius-activated transport with a field-enhanced gap $\Delta(B) = \Delta_0 + \gamma B$ with $\gamma = 1.1$ meV/T. This value is one order of magnitude larger than the bare Zeeman gap $\Delta = g\mu_B B$ (0.116 meV at 1 T). We therefore suggest that an exchange-enhanced mechanism is responsible for the field-induced gap opening.

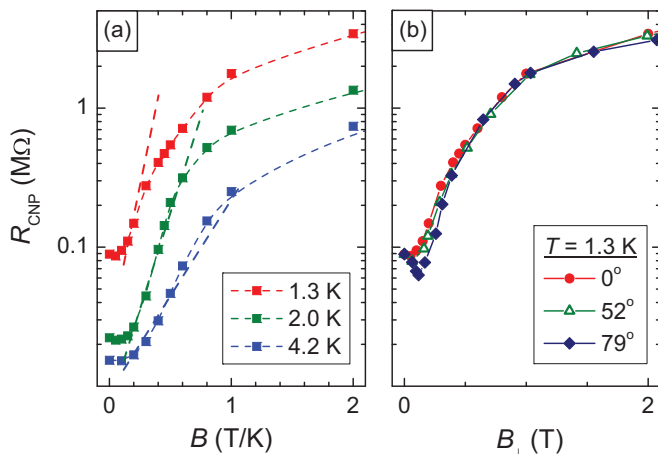


FIG. 3. (Color online) (a) R_{CNP} in a magnetic field perpendicular to the two-dimensional electron system plotted as a function of B/T for different temperatures. (b) R_{CNP} at 1.3 K in tilted magnetic fields plotted as a function of the perpendicular field component B_{\perp} .

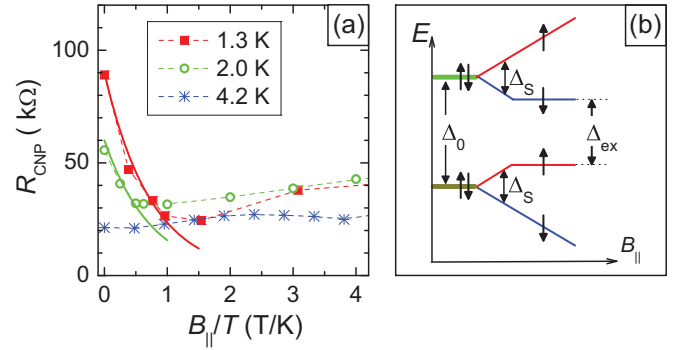


FIG. 4. (Color online) (a) Resistance at the CNP in a parallel magnetic field plotted as a function B/T . The solid lines show the expected resistance decrease, $R \propto \exp(-2\mu_B B/k_B B_{\parallel} T)$, scaling with the bare Zeeman energy. (b) Proposed scenario for the behavior in a parallel magnetic field: A gap Δ_0 present at 0 T closes due to spin splitting in both energy levels. An exchange mechanism prevents a further decrease of the gap for parallel fields above 2 T, and a finite gap $\Delta_{\text{ex}} = 0.25$ meV remains.

The scenario of an exchange-driven gap at the CNP is further supported by experiments in tilted magnetic fields shown in Fig. 3(b). The resistance at the CNP is governed by the perpendicular magnetic field B_{\perp} alone, consistent with a non-spin-related mechanism responsible for the gap at the CNP. This leads to an insulating phase of a quantum Hall insulator, as also proposed for single-layer and bilayer graphene.^{31,32}

Finally, we demonstrate that the bare Zeeman splitting at the CNP can be observed directly using a parallel magnetic field B_{\parallel} . As shown in Fig. 4(a), the resistance at the CNP decreases as a function of $B_{\parallel}/k_B T$, similar to a recent observation in a suspended BLG sample.³³ This decrease suggests that the gap is suppressed by a magnetic field, $\Delta = \Delta_0 - \Delta_{\parallel}(B)$. Assuming a simple Zeeman gap, $\Delta_{\parallel}(B) = 2\mu_B B_{\parallel}$, leads to a field dependence shown by the solid lines in Fig. 4(a). Indeed, the lines follow the experimental data up to $B_{\parallel}/T \approx 1$ T/K. Therefore, we can understand the field-induced gap closing at the CNP as a simple Zeeman splitting of the two spin-degenerate levels above and below the Fermi energy. For higher fields, the resistance remains constant, i.e., an exchange mechanism prevents the two energy levels from approaching and the gap remains open at an approximately constant value.

In conclusion, magnetotransport experiments on a two-probe suspended ABC-stacked trilayer graphene sample show the full lifting of the 12-fold degeneracy in the lowest Landau level. Performing a quantitative analysis on the distinctness of the related quantum Hall plateaus, we have determined an order for the appearance of the corresponding filling factors: $\nu = 6, 4, 0$ appear first, followed by $\nu = 3$, and finally $\nu = 1, 2, 5$. Furthermore, we have studied the opening of a gap at the CNP. Already at zero magnetic field we observe a gap $\Delta_0 = 0.38$ meV, which can be partly closed by the Zeeman effect in a parallel magnetic field. In contrast, in a perpendicular magnetic field, the gap at $\nu = 0$ was shown to increase linearly with field and to be an order of magnitude larger than the bare Zeeman gap. These facts point to a spin unpolarized ground state with an exchange-driven gap.

Part of this work has been supported by the Stichting Fundamenteel Onderzoek der Materie (FOM), with financial support from the Nederlandse Organisatie voor

Wetenschappelijk Onderzoek (NWO). We also thank the Zernike Institute for Advanced Materials and Nanoned for financial support.

*u.zeitler@science.ru.nl

- ¹K. S. Novoselov, A. K. Geim, S. V. Morozov, D. Jiang, M. I. Katsnelson, I. V. Grigorieva, S. V. Dubonos, and A. A. Firsov, *Nature (London)* **438**, 197 (2005).
- ²Y. Zhang, Y.-W. Tan, H. L. Stormer, and P. Kim, *Nature (London)* **438**, 201 (2005).
- ³K. S. Novoselov, E. McCann, S. V. Morozov, V. I. Fal'ko, M. I. Katsnelson, U. Zeitler, D. Jiang, F. Schedin, and A. K. Geim, *Nat. Phys.* **2**, 177 (2006).
- ⁴T. Taychatanapat, K. Watanabe, T. Taniguchi, and P. Jarillo-Herrero, *Nat. Phys.* **7**, 621 (2011).
- ⁵F. Zhang, H. Min, M. Polini, and A. H. MacDonald, *Phys. Rev. B* **81**, 041402 (2010).
- ⁶W. Bao, L. Jing, J. Velasco, Y. Lee, G. Liu, D. Tran, B. Standley, M. Aykol, S. B. Cronin, D. Smirnov, M. Koshino, E. McCann, M. Bockrath, and C. N. Lau, *Nat. Phys.* **7**, 948 (2011).
- ⁷A. Kumar, W. Escoffier, J. M. Poumirol, C. Faugeras, D. P. Arovas, M. M. Fogler, F. Guinea, S. Roche, M. Goiran, and B. Raquet, *Phys. Rev. Lett.* **107**, 126806 (2011).
- ⁸S. H. Jhang, M. F. Craciun, S. Schmidmeier, S. Tokumitsu, S. Russo, M. Yamamoto, Y. Skourski, J. Wosnitza, S. Tarucha, J. Eroms, and C. Strunk, *Phys. Rev. B* **84**, 161408 (2011).
- ⁹E. McCann and V. I. Falko, *Phys. Rev. Lett.* **96**, 086805 (2006).
- ¹⁰F. Guinea, A. H. Castro Neto, and N. M. R. Peres, *Phys. Rev. B* **73**, 245426 (2006).
- ¹¹M. Koshino and E. McCann, *Phys. Rev. B* **83**, 165443 (2011).
- ¹²A. A. Avetisyan, B. Partoens, and F. M. Peeters, *Phys. Rev. B* **81**, 115432 (2010).
- ¹³S. Yuan, R. Roldan, and M. I. Katsnelson, *Phys. Rev. B* **84**, 125455 (2011).
- ¹⁴M. Ezawa, *J. Phys. Soc. Jpn.* **76**, 094701 (2007).
- ¹⁵C. R. Dean, A. F. Young, I. Meric, C. Lee, L. Wang, S. Sorgenfrei, K. Watanabe, T. Taniguchi, P. Kim, K. L. Shepard, and J. Hone, *Nat. Nanotechnol.* **5**, 722 (2010).
- ¹⁶C. R. Dean, A. F. Young, P. Cadden-Zimansky, L. Wang, H. Ren, K. Watanabe, T. Taniguchi, P. Kim, J. Hone, and K. L. Shepard, *Nat. Phys.* **7**, 693696 (2011).
- ¹⁷K. I. Bolotin, K. J. Sikes, Z. Jiang, M. Klima, G. Fudenberg, J. Hone, P. Kim, and H. L. Stormer, *Solid State Commun.* **146**, 351 (2008).
- ¹⁸N. Tombros, A. Veligura, J. Junesch, J. J. van den Berg, P. J. Zomer, M. Wojtaszek, I. J. V. Marun, H. T. Jonkman, and B. J. van Wees, *J. Appl. Phys.* **109**, 093702 (2011).
- ¹⁹K. S. Novoselov, A. K. Geim, S. V. Morozov, D. Jiang, Y. Zhang, S. V. Dubonos, I. V. Grigorieva, and A. A. Firsov, *Science* **306**, 666 (2004).
- ²⁰P. Blake, E. W. Hill, A. H. C. Neto, K. S. Novoselov, D. Jiang, R. Yang, T. J. Booth, and A. K. Geim, *Appl. Phys. Lett.* **91**, 063124 (2007).
- ²¹J. Moser, A. Barreiro, and A. Bachtold, *Appl. Phys. Lett.* **91**, 163513 (2007).
- ²²A. M. Chang and D. C. Tsui, *Solid State Commun.* **56**, 153 (1985).
- ²³B. Tieke, R. Fletcher, U. Zeitler, A. K. Geim, M. Henini, and J. C. Maan, *Phys. Rev. Lett.* **78**, 4621 (1997).
- ²⁴F. Freitag, J. Trbovic, M. Weiss, and C. Schonenberger, *Phys. Rev. Lett.* **108**, 076602 (2012).
- ²⁵N. Tombros, A. Veligura, J. Junesch, M. H. D. Guimaraes, I. J. Vera-Marun, H. T. Jonkman, and B. J. van Wees, *Nat. Phys.* **7**, 697 (2011).
- ²⁶H. J. van Elferen, A. Veligura, E. V. Kurganova, U. Zeitler, J. C. Maan, N. Tombros, I. J. Vera-Marun, and B. J. van Wees, *Phys. Rev. B* **85**, 115408 (2012).
- ²⁷L. M. Lifshitz and A. M. Kosevich, *Zh. Eksp. Teor. Fiz.* **29**, 730 (1955) [*Sov. Phys. JETP* **2**, 636 (1956)].
- ²⁸F. Zhang, D. Tilahun, and A. H. MacDonald, *Phys. Rev. B* **85**, 165139 (2012).
- ²⁹Y. Barlas, R. Cote, and M. Rondeau, *Phys. Rev. Lett.* **109**, 126804 (2012).
- ³⁰M. Koshino and E. McCann, *Phys. Rev. B* **79**, 125443 (2009).
- ³¹Z. Jiang, Y. Zhang, H. L. Stormer, and P. Kim, *Phys. Rev. Lett.* **99**, 106802 (2007).
- ³²J. G. Checkelsky, L. Li, and N. P. Ong, *Phys. Rev. Lett.* **100**, 206801 (2008).
- ³³A. Veligura, H. J. van Elferen, N. Tombros, J. C. Maan, U. Zeitler, and B. J. van Wees, *Phys. Rev. B* **85**, 155412 (2012).